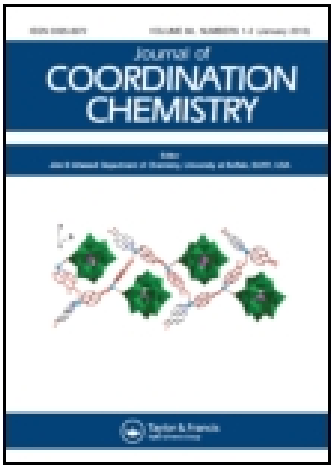

Journal of Coordination Chemistry
Publication details, including instructions for authors and subscription information:
http://www.tandfonline.com/loi/gcoo20

Structural characterization and physicochemical properties of quercetin-Pb complex

R. Ravichandran[a], M. Rajendran[a] & D. Devapiriam[a]
[a] Department of Chemistry, Centre for Research and Post Graduate Studies in Chemistry, N. M. S. S. Vellaichamy Nadar College, Madurai, India
Accepted author version posted online: 17 Apr 2014.Published online: 20 May 2014.

To cite this article: R. Ravichandran, M. Rajendran & D. Devapiriam (2014) Structural characterization and physicochemical properties of quercetin-Pb complex, Journal of Coordination Chemistry, 67:8, 1449-1462, DOI: 10.1080/00958972.2014.915317

To link to this article: http://dx.doi.org/10.1080/00958972.2014.915317

Journal of Coordination Chemistry, 2014
Vol. 67, No. 8, 1449–1462, http://dx.doi.org/10.1080/00958972.2014.915317

Structural characterization and physicochemical properties of quercetin–Pb complex

R. RAVICHANDRAN, M. RAJENDRAN* and D. DEVAPIRIAM

Department of Chemistry, Centre for Research and Post Graduate Studies in Chemistry, N. M. S. S. Vellaichamy Nadar College, Madurai, India

(*Received 18 November 2013; accepted 26 February 2014*)

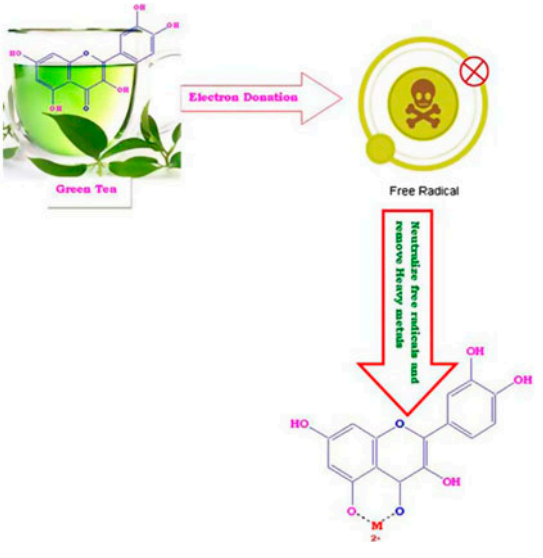

Flavonoids are a large group of ubiquitous molecules synthesized by plants. These molecules possess antioxidant activities which prevent free radical damage to biological molecules and can also be metal chelators. This article describes the synthesis of a Pb(II)–quercetin complex and characterization by UV–visible, infrared, ^{1}H nuclear magnetic resonance spectroscopy, thermogravimetric analysis, and differential thermal analysis. The formation of quercetin and Pb(II) complex ratio 1 : 1 was confirmed by UV–visible spectroscopy. The composition of the complex does not change with pH. Antimicrobial activities were evaluated by using Gram-positive and Gram-negative bacteria. The antioxidant properties of quercetin and the complex was evaluated by using 2,2′-diphenyl-1-picrylhydrazyl radical scavenging method. The quercetin–Pb complex was less effective than quercetin in antimicrobial and antioxidant activity.

*Corresponding author. Email: mrrajendran64@yahoo.com

Keywords: Quercetin; Quercetin–Pb complex; Thermogravimetry; Antioxidant; Antimicrobial activity

1. Introduction

Metal toxicity occurs due to essential metal overload problems or exposure to heavy metals from various sources. Metals and metal compounds interfere with functions of various organ systems of our body like the central nervous system, liver, and kidneys. [1–3]. Many available chelating agents have serious side effects [4]. There are number of chelating agents available, but their side effects are significant. Calcium disodium ethylenediamine tetraacetic acid ($CaNa_2EDTA$) is the most used chelating agent, complexing a wide variety of metal ions and is used clinically despite associated risks. $CaNa_2EDTA$ cannot pass through cellular membranes and therefore its use is restricted in removing metal ions in the extracellular fluid. Similarly, conventionally used meso-2,3-dimercaptosuccinic acid and deferoxamine were used as a drug for lead metal poisoning [5, 6]. These chelating drugs are generally well tolerated with a few cases where side effects include ophthalmic and auditory toxicity, bacterial and fungal infections, alterations in blood histology, allergic and skin reaction, and a few reported adverse effects on lungs, kidneys, and nervous system [7]. Free radical-induced damage occurs by lead poisoning through direct formation of reactive oxygen species including singlet oxygen, hydrogen peroxides, and hydroperoxides or by depletion of the cellular antioxidant pool [8]. The sulphydryl groups of natural antioxidant glutathione bind toxic metals such as arsenic and mercury [9]. An organism exposed to lead has significantly lower levels of glutathione, with respect to the control groups, which may in turn enhance the toxicity of other metals [10, 11]. Quercetin is a natural antioxidant with vitamin P activity, which can strengthen blood vessel walls and improve their tone, and can increase the sensitivity and conductivity of the optic nerve [12, 13]. Quercetin is the most abundant bioflavonoid found in vegetables and fruits [14, 15]. Quercetin can strongly chelate metal cations with 3-hydroxy-4-keto group, 5-hydroxy-4-keto group, and ortho-dihydroxyl (catechol) group of the B ring [16]. Chelation between quercetin and transition metals has attracted attention because the complexes formed have higher antioxidant and antitumor activities [17, 18]. Metal chelation is widely considered as another mechanism of antioxidant activity of flavonoids. Metal ions play an important role in many biological systems with various biomolecules, related to essential physiological activities in the human organism. The interaction of quercetin with metal ions may also change the antioxidant properties and biological effects of quercetin. Biological activity of a ligand can be increased when coordinated or mixed with suitable metal ion, because of its ability to act as free radical acceptor [19, 20]. We focused on a lead complex because of its toxicity and widespread presence in the environment. All lead compounds are considered cumulative poisons; lead poisoning can affect the gastrointestinal track and nervous system [21, 22]. Heavy metals may be eliminated from biological systems with the help of a natural chelator. The stability of a quercetin–lead chemical, thermal, and biological behaviors were studied in this article.

2. Materials and methods

2.1. *Chemicals and reagents*

Quercetin (3,3′,4′,5,7-pentahydroxyflavone) and 2,2′-diphenyl-1-picrylhydrazyl radical (DPPH) were purchased from Sigma Aldrich Chemicals, USA. Lead nitrate was obtained from Merck, India. All other reagents and solvents were of analytical grade, chemically pure and used as received.

2.2. *Instrumental study*

UV–visible spectra of free and complexed quercetin were recorded on a SHIMADZU-1800 model UV–visible spectrophotometer (S. No.: A11454806363). FTIR spectroscopic studies of the quercetin and its complex were determined by a SHIMADZU from 400 to 4000 cm^{-1}. ^{1}H nuclear magnetic resonance (NMR) spectrum was recorded using a BRUKER 300 MHZ Model instrument at Madurai Kamaraj University, Madurai. Thermogravimetric analysis (TGA) and differential thermal analysis (DTA) of the quercetin metal complex were analyzed using an SII Exstar 6000 model TGA/DTA analyzer. Electrochemistry for quercetin and the quercetin-lead complex was carried out with a CHI660E model instrument.

2.3. *Determination of stability constant*

Job's method was used to determine the stoichiometric ratio and stability constant of the complex. The solutions were prepared by mixing solutions of both components with equal molar concentration (1×10^{-3} M) in ratios varying from 1 : 9 to 9 : 1. The absorbance of quercetin was measured at 372 nm [23, 24].

2.4. *Synthesis of quercetin–lead complex*

In a 50 mL round bottom flask provided with an electromagnetic stirrer, solid quercetin (0.01 M) and 20 mL ethanol were combined until the quercetin was completely dissolved. To the yellow solution, when solid lead nitrate (0.02 M) was added quickly, the color of the solution changed to dark green and stirring was continued for 2 h at room temperature. After stirring, the reaction mixture was filtered and the filtrate evaporated slowly at room temperature to obtain a solid product. Unreactive reagents were removed by washing with water [25].

2.5. *Electrochemical reactions of quercetin and quercetin–Pb complex*

Cyclic voltammetric measurements were carried out with a ALS/CH Instruments model 660E Electrochemical Analyzer. All experiments were performed at room temperature (25 °C) in a conventional three-electrode system, equipped with a glassy carbon working electrode (3.0 mm), a sodium chloride saturated Ag/AgCl electrode as the reference electrode, and a platinum wire as the counter electrode. Quercetin and the quercetin–lead complex (0.01 M) were added to the phosphate buffer saline solution (pH 7.2), then the electrodes are connected to the instrument and the electrochemical cell was filled with the electrolyte solution. Cyclic voltammetry were performed at 100 mV scan rate, and the

potentials were reported as GCE *versus* Ag/AgCl electrode. The experiment was repeated every time the working electrode was polished with micro-polish powder (0.05 μM). The measurement cell was purged with argon for 5 min prior to each experiment, and then a blanket of argon was maintained during the experiment [26].

2.6. *DPPH assay*

DPPH assay is based on measurement of the scavenging ability of antioxidants towards the stable radical 2,2′-diphenyl-1-picrylhydrazyl. DPPH, which shows absorbance at 540 nm, is reduced to the corresponding hydrazine when it reacts with hydrogen donors. DPPH assay is considered as a valid and easy assay to evaluate the radical scavenging activity of antioxidants [27]. The antioxidant activities of quercetin and its complex were studied in ethanol [28]. The reduction of DPPH (50 μM) by quercetin and quercetin–lead complex was monitored at 540 nm in ethanol. The spectrophotometer reading was recorded for 30 min. Absorbance at 540 nm was recorded every 2 min. DPPH (50 μM) in ethanol served as control [29].

2.7. *Biological activity*

The antimicrobial activities of quercetin and quercetin–Pb complex were tested *in vitro* by the disk method. Gram-positive and Gram-negative bacteria were used and streptomycin was the standard drug. Bacterial culture (0.1 mL) was inoculated on an agar gel plate and quercetin and complex containing disks (10 μL) were placed on the plates. The plates were incubated at 30 °C for 24 h and observed for antibacterial activity [30, 31].

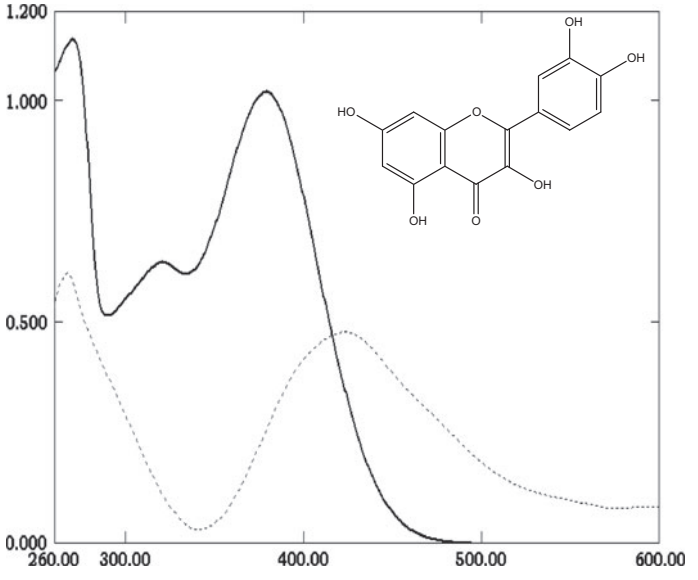

Figure 1. UV–vis absorption spectra of quercetin (solid line) and quercetin–Pb complex (dotted line). Inserted figure is the structure of quercetin.

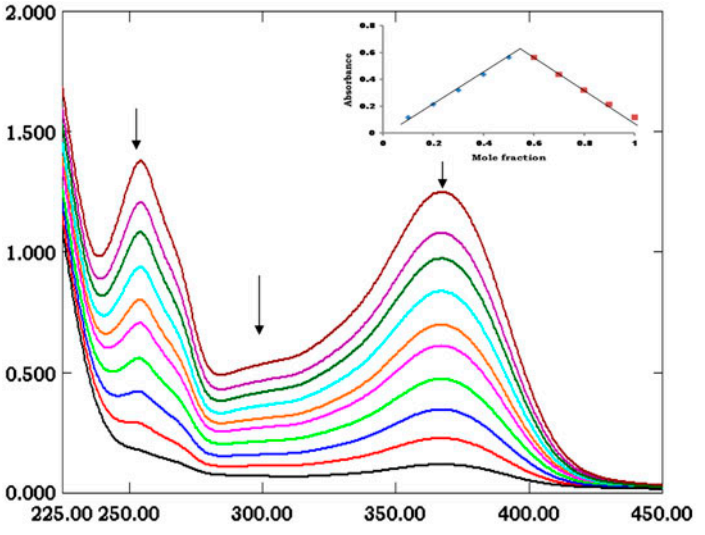

Figure 2. UV–visible spectral curves of quercetin with Pb(II). The arrow shows the intensity decreases with increasing the concentration (5×10^{-5}–4×10^{-4}) of Pb(II). The insert figure shows quercetin and Pb(II) form quercetin–Pb complex by 1 : 1 ratio.

3. Results and discussion

3.1. *Determination of stability constant by Job's method*

Figure 1 shows UV–vis spectra of free quercetin and the quercetin–Pb complex. The quercetin–Pb complex spectrum was red-shifted from quercetin, due to metal orbital and quercetin OH group overlap. Complex formation between quercetin and lead was confirmed through these spectra. Quercetin–Pb complex UV–vis spectrum lacked one peak of free quercetin, due to the formation of complex in ring-C. The quercetin structure has OH groups attached to ring structures that can be involved in chelation of metals. In order to test the complex stability, a series of stoichiometry studies were performed using Job's method. The insert (figure 2) indicates that complex between quercetin and lead was 1 : 1 stoichiometry [32]. Increasing addition of Pb(II) to the quercetin solution decreased the intensity of quercetin absorbance (figure 2). This observation showed that Pb(II) binds with quercetin [33, 34]. The equilibrium constant of quercetin–Pb complex was determined in acetate buffer (pH 4.4) and also in phosphate buffer (pH 7.4). The stability constant of quercetin–Pb complex in phosphate buffer was larger (9×10^6) than in acetate buffer (1.4×10^6). The results showed that the complex was stable at pH 7.4 due to quercetin in basic medium which was readily deprotonated to make the complex with lead.

3.2. *Transitional behavior of molecular quercetin and Pb–quercetin complex*

Electronic spectra of quercetin and the quercetin–lead complex were recorded in phosphate buffer (pH 7.4) solution. Quercetin shows two main peaks at 374 nm (band I) and 256 nm (band II), band-I at 374 nm corresponds to the cinnamoyl system of the B ring and absorbance at 256 nm arises from the benzoyl system of ring A. The quercetin–Pb complex

Table 1. IR data of quercetin and quercetin–Pb complex.

Functional group	Quercetin	Quercetin–Pb(II) complex
C=O	1670.24	–
Aromatic C–H	1614.31, 1512.04, 1458.02	1606.59, 1514.62, 1140.00
C–OH deform	1244.00	1267
C–OH stretching	1164.00	1164.00

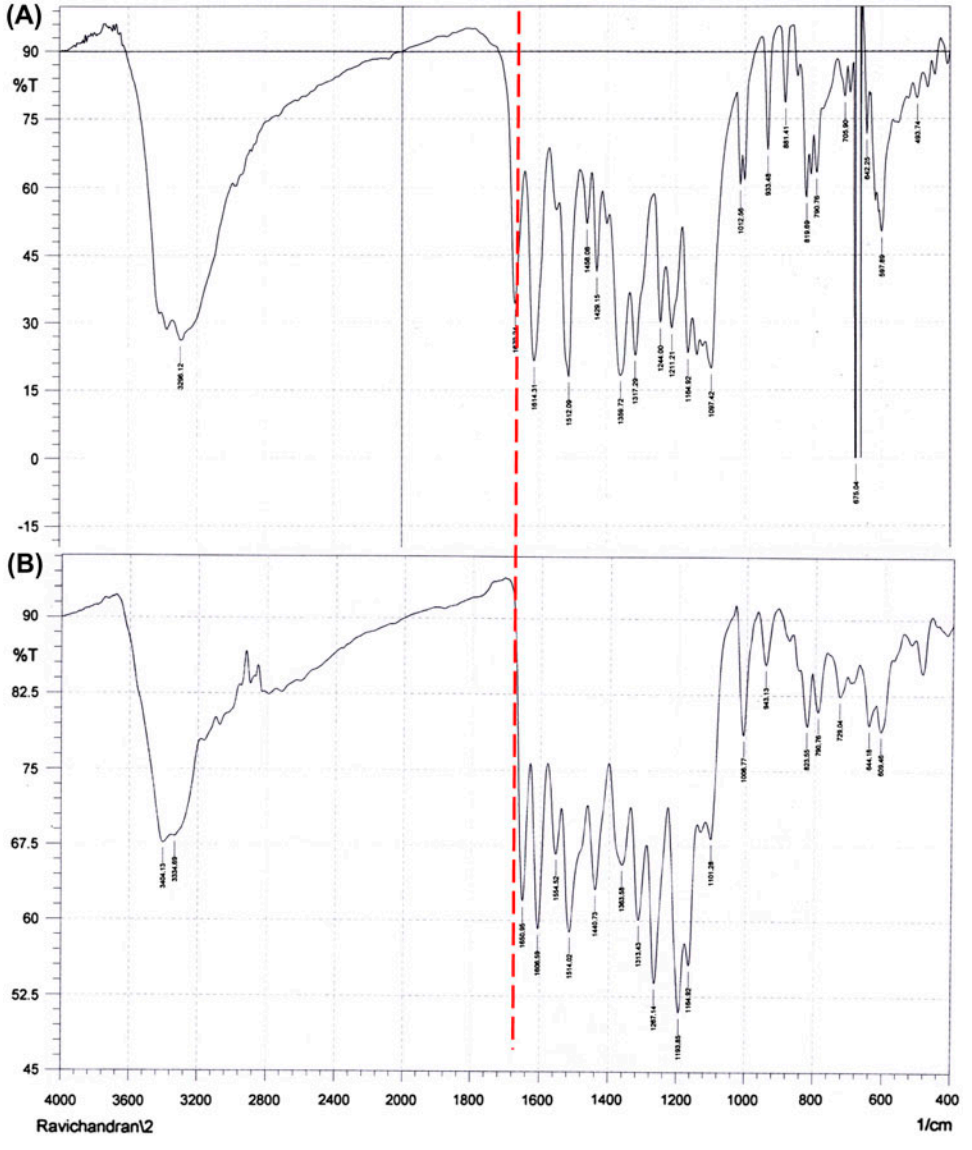

Figure 3. IR spectra of (A) quercetin and (B) quercetin–Pb complex.

shifted to longer wavelength than quercetin as shown in figure 2 [35]. Comparative spectral analysis of quercetin and quercetin–Pb complex showed that hydroxyl substitution at C-5 in the A-ring and keto group in the C-ring was responsible for a spectral shift in the visible region after binding with lead. After chelation of Pb(II), quercetin peak was shifted to longer wavelength by 49 and 8 nm, respectively. The bathochromic shift was from the extension of the conjugation within the quercetin–Pb complex.

3.3. *Quercetin–Pb complex characterization by FTIR*

FTIR spectral data of quercetin and quercetin–Pb(II) complex are listed in table 1. The characteristic C=O stretch of the quercetin keto group at 1670 cm^{-1} shifted to lower wavenumber in the complex (figure 3). Coordination occurred through the keto group oxygen and the 3-OH or 5-OH group deprotonation to form Pb(II) oxygen bonds. A O–H stretch as a broad peak at 3200–3400 cm^{-1} indicates water molecules, also confirmed by thermal analysis.

3.4. *Quercetin–Pb complex characterization by ^{1}H NMR*

Quercetin and its complex were characterized by ^{1}H NMR spectra; the observed chemical shifts are listed in table 2. In the ^{1}H NMR spectrum of quercetin, the 5–OH was a singlet at 12.4 ppm, but in the quercetin–Pb complex the 5-OH peak was absent (figure 4). Remaining signals like 7-OH, 3-OH, and dihydroxyl groups are slightly shifted upfield compared to free quercetin, because spin–orbital coupling occurred due to complex formation. Thus, we conclude that metal complexation takes place at 5-OH and carbonyl. The proposed structure between quercetin and lead is presented in scheme 1.

3.5. *Thermal behavior of molecular quercetin and quercetin–Pb complex*

The thermal stabilities of quercetin and its complex were determined by TGA from 0 to 600 °C under nitrogen with a heating rate of 20 °C min^{-1}. The main aim of the thermal studies is to assign the number and nature of water present and thermal stability of quercetin and its complex. Quercetin and its complex were not volatile and decomposition commences after 100 °C. Figure 5 shows quercetin and its complex displaying two main decompositions. The first dehydration starts from 0 to 100 °C. The second dehydration starts from 140 to 250° C with corresponding 30% of mass loss value from coordinated water [36, 37]. DTA peaks for the quercetin and its complex showed exothermic peaks that agree with mass losses observed in TGA, a sharp peak at 300–400 °C showing crystalline

Table 2. ^{1}H NMR data for quercetin and its Pb(II) complex.

–OH group	Quercetin	Quercetin–Pb(II) complex
5-OH	12.4	–
7-OH	10.9	10.45
3-OH	9.09	9.06
4′-OH	9.69	8.06
3′-OH	7.6	7.73

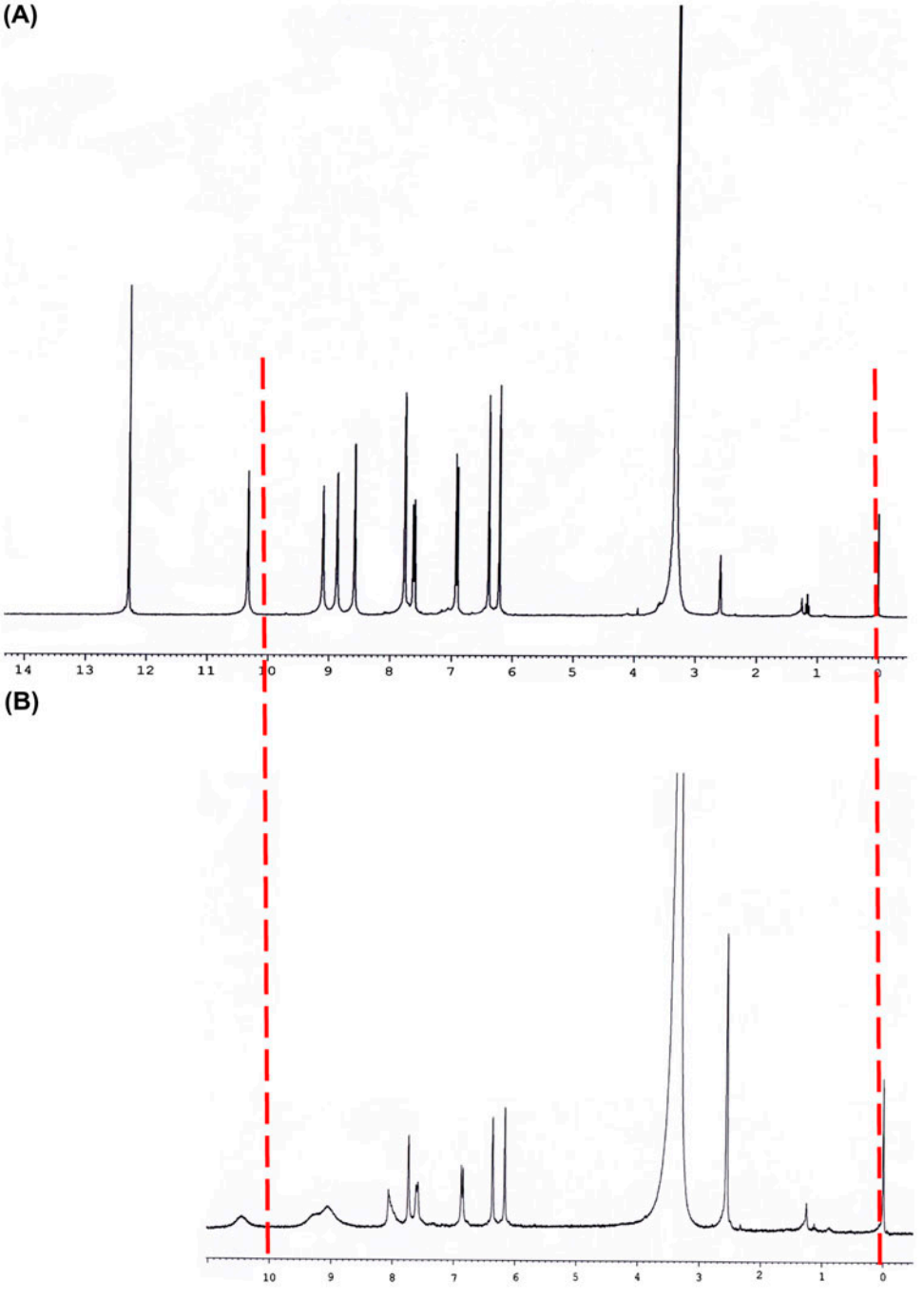

Figure 4. ^{1}H NMR spectra of (A) quercetin and (B) quercetin–Pb complex.

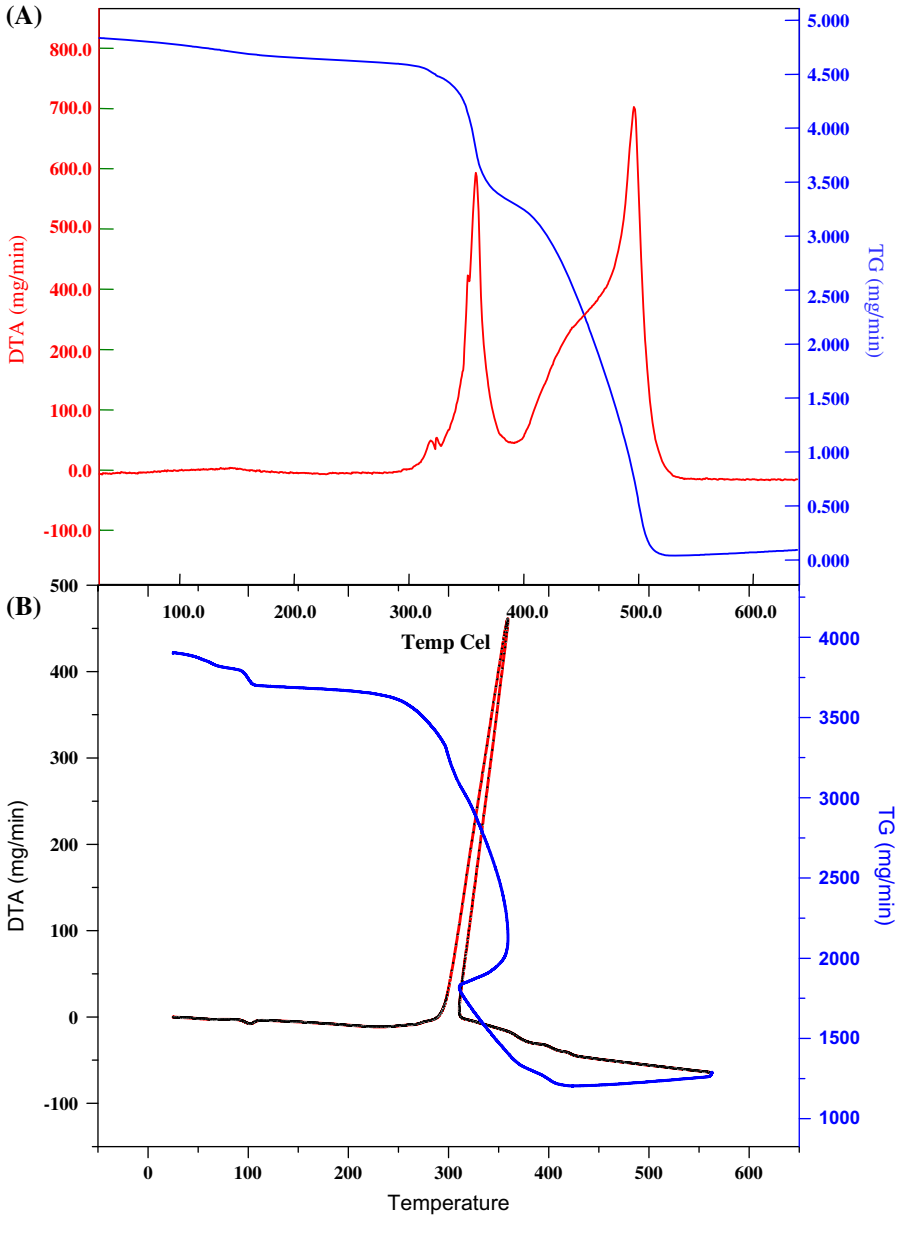

Figure 5. TGA and DTA curve of the (A) quercetin and (B) quercetin–lead complex (sample mass 5 mg; heating rate 20 °C min^{-1}).

water in the complex. A sharp exothermic peak was observed in quercetin at 300–500 °C, due to decomposition of organic matter.

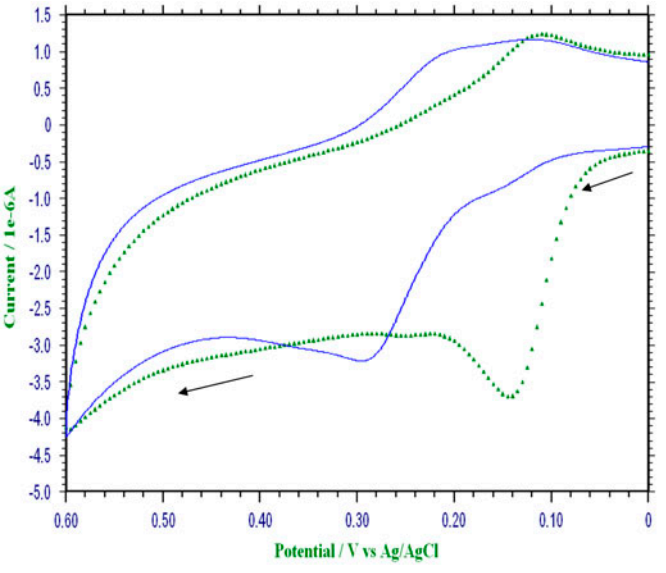

Figure 6. Cyclic voltammograms of (0.01 M) quercetin (dotted line) and quercetin–Pb complex (solid line) in phosphate buffer saline (pH 7.2) at 100 mV scan rate.

Table 3. Anodic and cathodic peak potentials (E_{pa} and E_{pc}) and the corresponding ΔE_p of quercetin and quercetin–Pb complex.

		Electrochemical parameter			
Sl. No.	Compounds	E_{pa} (V)	E_{pc} (V)	ΔE_p (V)	$E_{1/2}$ (V)
1	Quercetin	0.143	0.108	0.035	0.125
2	Quercetin–Pb complex	0.295	0.205	0.09	0.25

3.6. *Redox behavior of quercetin and its lead complex*

The electrochemical behaviors of quercetin and its lead complex show that complex redox properties completely vary from free quercetin. Figure 6 shows a cyclic voltammogram of quercetin (dotted line) and its lead complex (solid line) in phosphate buffer saline (pH 7.2). Quercetin anodic and cathodic peak potentials were observed at +0.143 and +0.108 V, respectively. Redox potential values are also confirmed by differential pulse voltammetry. The quercetin–lead complex shows higher redox potential than free quercetin, +0.295 and +0.205 V, for anodic and cathodic peak potentials, respectively. . The oxidation potentials of quercetin and complex are +0.143 and +0.295 V, respectively (table 3) and the order of free radical quenching by quercetin was higher than the quercetin–Pb complex. Lower oxidation potential has higher antioxidant efficiency. Similarly, the inhibition rates of antimicrobials also show this trend. It may be concluded that lower oxidation potential more easily donates electron to free radical, similar for antimicrobial activity.

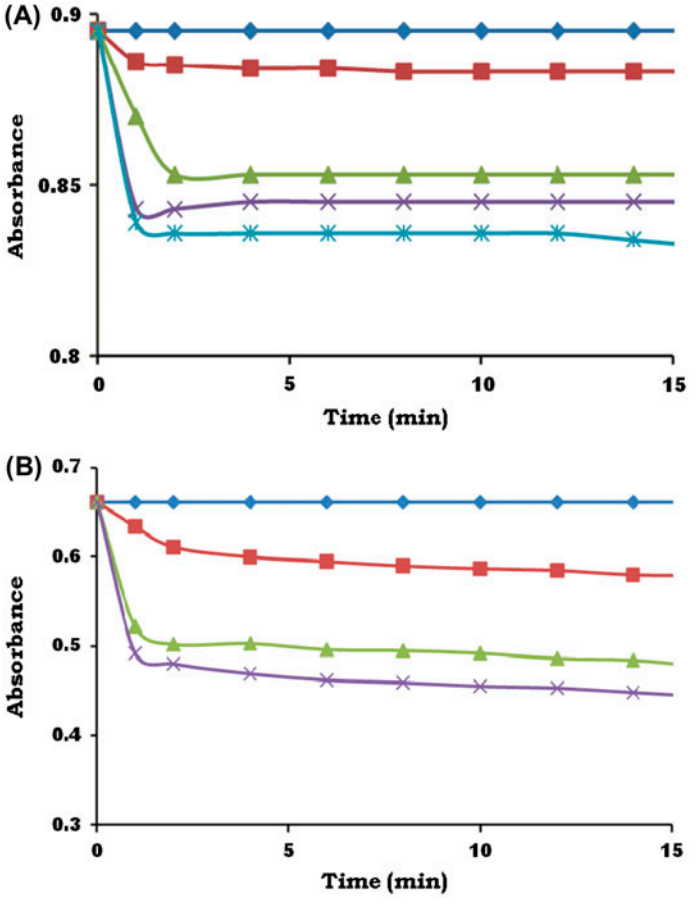

Figure 7. Decrease in absorbance of DPPH (λ 515 nm) solution in the presence of various concentrations of (A) quercetin–Pb complex (■■■ 5 μM, ▲▲▲ 10 μM, xxx 15 μM, ***20 μM) and control DPPH (♦♦♦ 50 μM) and (B) quercetin with three (■■■ 5 μM, ▲▲▲ 10 μM, xxx 15 μM) concentrations. The kinetics of scavenging effects were determined by 15 min.

Table 4. Antimicrobial activity of quercetin and quercetin–Pb complex.

		Zone of inhibition (mm)	
Compound	Concentration (M)	*E. coli*	*S. aureus*
Quercetin	0.01	14	19
	0.001	R	R
	0.0001	R	R
Quercetin–Pb complex	0.01	R	R
	0.001	R	R
	0.0001	R	R
Standard drug	10 μg	17	18

*R – resistant (no activity).

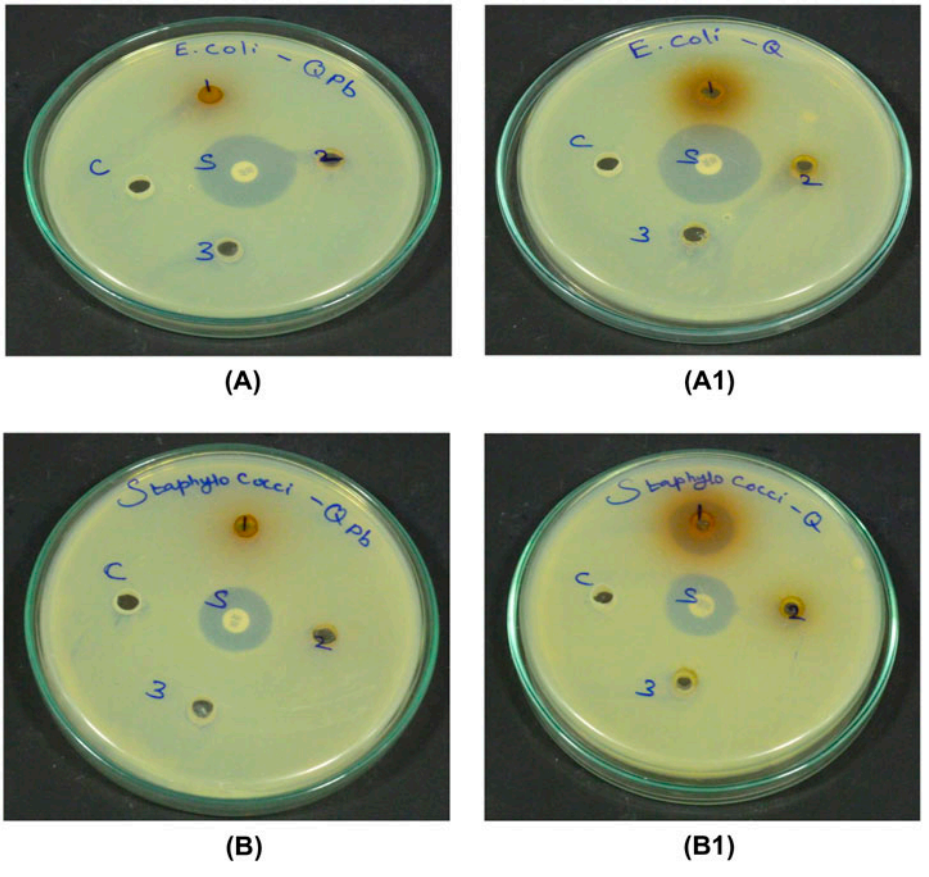

Figure 8. The zone of inhibition of quercetin (A1), (B1) quercetin–Pb(II) complex (A), (B) against Gram-positive strain *E. coli* and Gram-negative strain *S. aureus* for different concentrations (1 = 0.01, 2 = 0.001, and 3 = 0.0001 M), S = standard drug (ampicillin (10 µg)) and C = control DMSO only.

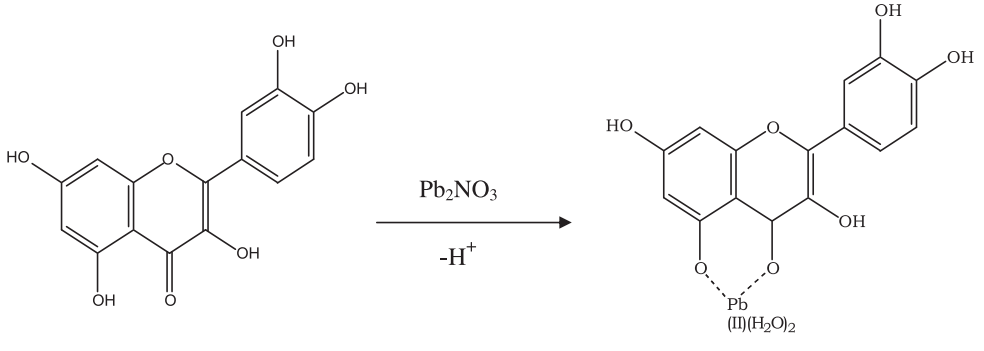

Scheme 1. Schematic representation of quercetin–Pb(II) complex.

3.7. *Antioxidant activity*

The results of radical scavenging analysis by quercetin and complex are shown in figure 7, both scavenged DPPH free radical effectively. The radical scavenging activity of quercetin was higher than that of the quercetin–Pb complex; quercetin radical scavenging activity was 4.08, 23.90, and 30.10% for 5, 10, and 15 μM, respectively. For quercetin–Pb(II) complex, scavenging was 1.2, 4.69, 5.8, and 6.25% for 5, 10, 15, and 20 μM, respectively. Perhaps, the lower activity of quercetin–Pb complex arises from lower number of hydroxyl groups [38]. The electrochemical results are also correlated to antioxidant activity, and quercetin–Pb complex has higher oxidation potential than quercetin. Lower potential of quercetin readily leaves an electron to DPPH, reducing it to the corresponding non-radical species.

3.8. *Antimicrobial activity*

Quercetin and quercetin–Pb complex were tested against *Escherichia coli* and *Staphylococcus aureus* microorganisms at 0.01, 0.001, and 0.0001 M. After incubation, the zone of inhibition was calculated (table 4). Quercetin shows (figure 8) good antimicrobial activity both in Gram-positive (*E. coli*) and Gram-negative bacteria (*S. aureus*), when compared to quercetin–Pb complex, in the same concentrations. The quercetin–Pb complex has no activity on the strains, due to change of physicochemical properties of quercetin in the complex. Quercetin has zone of inhibition of 14 and 19 mm, respectively, against *E. coli* and *S. aureus* [39–41].

4. Conclusion

Both quercetin and quercetin–Pb complex have antioxidant activities, with quercetin higher than complex. The antioxidant results indicate that electron donating ability was lower in quercetin–Pb complex. Combined spectroscopic and thermal studies have been used to determine the preferential complexing site of quercetin through 5-hydroxyl and carbonyl sites. The stability of quercetin–Pb complex was very high, indicating that quercetin can be a natural metal chelator of toxic metals. Thermal studies confirmed that stability of complex was very high. The oxidation potential of quercetin is lower than its complex. These results correlated with antioxidant efficiency and antimicrobial study on Gram-positive (*E. coli*) and Gram-negative (*S. aureus*) bacteria.

Acknowledgement

The authors are thankful to the University Grants Commission of India Major Research Project (File No. 39-731/2010) for their financial support.

References

[1] G.T. Morgan, H.D.K. Drew. *J. Chem. Soc., Trans.*, 1456 (1920).
[2] O. Andersen. *Chem. Rev.*, **99**, 2683 (1999).
[3] M.M. Jones. In *Coordination Chemistry: A Century of Progress*, G.B. Kauffman (Ed.), pp. 58–67, The American Chemical Society, Washington, DC (1994).
[4] K.A. Winship. *Toxicol. Rev.*, **12**, 177 (1993).

[5] C.R. Angle. In *Toxicology of Metals*, L.W. Chang (Ed.), pp. 827–834, CRC Press, Boca Raton, FL (1996).
[6] A. Kuzniar, M. Kopacz, D. Nowak. *J. Coord. Chem.*, **61**, 1005 (2008).
[7] D.N. Guha Mazumder, U.C. Ghoshal, J. Saha, A. Santra, B.K. De, A. Chatterjee, S. Dutta, C.R. Angle, J.A. Centeno. *Clin. Toxicol.*, **36**, 683 (1998).
[8] N. Ercal, H. Gurer-Orhan, N. Aykin-Burns. *Curr. Top. Med. Chem.*, **1**, 529 (2001).
[9] H. Gurer, N. Ercal. *Free Radical. Biol. Med.*, **29**, 927 (2000).
[10] A.A. Hunaiti, M. Soud. *Sci. Total Environ.*, **248**, 45 (2000).
[11] L.G. Donracheva, N.B. Melnikova, I.A. Pegova, A.A. Volkov, G.A. Domrachev, O.V. Kolchik. *Chem. J.*, **42**, 564 (2008).
[12] S.B. Bukhari, S. Memon, M.M. Tahir, M.I. Bhanger. *J. Mol. Struct.*, **892**, 39 (2008).
[13] S.J.S. Flora. *Free Radical. Biol. Med.*, **51**, 257 (2011).
[14] P.A. Omololu, J.B.T. Rocha, I.J. Kade. *Exp. Toxicol. Pathol.*, **63**, 249 (2011).
[15] J.P. Cornard, J.C. Merlin. *J. Mol. Struct.*, **653**, 381 (2003).
[16] S. Sun, W. Chen, W. Cao, F. Zhang, J. Song, C. Tian. *J. Mol. Struct.*, **860**, 40 (2008).
[17] M. Leopoldini, N. Russo, S. Chiodo, M. Toscano. *J. Agric. Food Chem.*, **54**, 6343 (2006).
[18] J. Zhang, L. Ma, F. Zhang, Z. Zhang, L. Li, S. Wang. *J. Coord. Chem.*, **65**, 239 (2012).
[19] J. Zhou, L. Wang, J. Wang, N. Tang. *J. Inorg. Biochem.*, **83**, 41 (2001).
[20] R.F.V. Souza, W.F.D. Giovani. *Spectrochim. Acta Part A*, **61**, 1985 (2005).
[21] R. Ravichandran, M. Rajendran, D. Devapiriam. *Food Chem.*, **146**, 472 (2014).
[22] K. Zhang, W.H. Cheung, M. Valix. *Chemosphere*, **60**, 1129 (2005).
[23] R.F.V. Souza, W.F.D. Giovani. *Spectrochim. Acta Part A*, **61**, 1985 (2005).
[24] Q.K. Panhwar, S. Memon. *J. Coord. Chem.*, **64**, 2117 (2011).
[25] S.B. Bukhari, S. Memon, M. Mahroof-Tahir, M.I. Bhanger. *Spectrochim. Acta Part A*, **71**, 1901 (2009).
[26] A. Zhou, S. Kikandi, O.A. Sadik. *Electrochem. Commun.*, **9**, 2246 (2007).
[27] A. Seyoum, K. Asres, F.K. El-Fiky. *Phytochemistry*, **67**, 2058 (2006).
[28] O. Dangles, G. Fargeix, C. Dufour. *J. Chem. Soc., Perkin Trans. 2*, 1387 (1999).
[29] C. Cimpoiu, V.M. Cristea, A. Hosu, M. Sandru, L. Seserman. *Food Chem.*, **127**, 1323 (2011).
[30] O.N. Irobi, M. Moo-Young, W.A. Anderson. *Int. J. Pharm.*, **34**, 87 (1996).
[31] M.A. Carvalho, B.C. Souza, R.E.F. Paiva, F.R.G. Bergamini, A.F. Gomes, F.C. Gozzo, W.R. Lustri, A.L.B. Formiga, G. Rigatto, P.P. Corbi. *J. Coord. Chem.*, **65**, 1700 (2012).
[32] P. Ryan, M.J. Hynes. *J. Coord. Chem.*, **61**, 3711 (2008).
[33] L. Dangleterre, J.P. Cornard, L. Lapouge. *Polyhedron*, **27**, 1581 (2008).
[34] G.V. Ferrari, M.P. Montaña, F.C.D. Dimarco, N.B. Debattista, N.B. Pappano, W.A. Massad, N.A. García. *J. Photochem. Photobiol. B*, **124**, 42 (2013).
[35] A.A. Ansari. *J. Coord. Chem.*, **61**, 3869 (2008).
[36] Q.K. Panhwar, S. Memon. *J. Coord. Chem.*, **65**, 1130 (2012).
[37] S. Dowling, F. Regan, H. Hughes. *J. Inorg. Biochem.*, **104**, 1091 (2010).
[38] D. Procházková, I. Boušová, N. Wilhelmová. *Fitoterapia*, **82**, 513 (2011).
[39] N. Dharmaraj, P. Viswanathamurthi, K. Natarajan. *Transition Met. Chem.*, **26**, 105 (2001).
[40] B. Roopashree, V. Gayathri, H. Mukund. *J. Coord. Chem.*, **65**, 1354 (2012).
[41] S.C. Singh, N. Gupta, R.V. Singh. *Indian J. Chem.*, **34A**, 733 (1995).